Talanta 81 (2010) 1063–1068

Contents lists available at ScienceDirect

Talanta

journal homepage: www.elsevier.com/locate/talanta

Synthesis of Pt/ionic liquid/graphene nanocomposite and its simultaneous determination of ascorbic acid and dopamine

Fenghua Li, Jia Chai, Huafeng Yang, Dongxue Han, Li Niu*

Engineering Laboratory for Modern Analytical Techniques, w/o State Key Laboratory of Electroanalytical Chemistry, Changchun Institute of Applied Chemistry, and Graduate University of the Chinese Academy of Sciences, Chinese, Academy of Sciences, Renmin St. 5625, Changchun 130022, Jilin, PR China

ARTICLE INFO

Article history:
Received 23 October 2009
Received in revised form 27 January 2010
Accepted 28 January 2010
Available online 6 February 2010

Keywords:
Graphene sheets
Platinum nanoparticles
Ionic liquid
Ascorbic acid
Dopamine

ABSTRACT

A water-soluble and electroactive composite – Pt nanoparticles/polyelectrolyte-functionalized ionic liquid (PFIL)/graphene sheets (GS) nanocomposite was synthesized in one pot. The structure and composition of the Pt/PFIL/GS nanocomposite were studied by means of ultraviolet–visible (UV–vis) and X-ray photoelectron spectra (XPS). Scanning electron microscopy (SEM) and transmission electron microscope (TEM) images reveal Pt nanoparticles are densely dispersed on the transparent thin PFIL-functionalized graphene sheets. The obtained Pt/PFIL/GS nanocomposite-modified electrode was fabricated to simultaneously determine ascorbic acid (AA) and dopamine (DA) by cyclic voltammetry. It is worthwhile noting that the difference between the two peak potentials of AA and DA oxidation is over 200 mV, which leads to distinguishing AA from DA. The detection of increasing concentrations of AA in the presence of DA and the oxidation of continuous addition of DA in the presence of AA were also studied using differential pulse voltammetry. The proposed sensor in real sample analysis was also examined in human urine samples. Three independent oxidation peaks appear in urine sample containing AA and DA. Therefore, the Pt/PFIL/GS nanocomposite might offer a good possibility for applying it to routine analysis of AA and DA in clinical use.

1. Introduction

Simultaneous determination of ascorbic acid (AA) and dopamine (DA) is a problem of critical importance in field of neurochemistry and biomedical chemistry [1]. Both, AA and DA, are compounds that can be determined by electrochemical methods based on anodic oxidation [2]. However, a major problem is that the oxidation peaks of AA and DA appear almost at the same potential at an unmodified electrode, which results in overlapping voltammetric responses making their discrimination highly difficult [3]. Recently, carbon based electrode materials such as: screen-printed carbon electrodes [4], ordered mesoporous carbons [5], carbon fiber microelectrodes [6], carbon nanotubes based materials [7], etc., have been applied to simultaneous electrochemical determination of AA and DA.

Graphene, a "rising-star" carbon material, has great promise for potential applications in many fields such as nanoelectronics, sensors, nanomaterials, and so on [8]. However, graphene sheets, unless well separated from each other, tend to form irreversible agglomerates or even restack to form graphite through *van der Waals* interactions. Therefore, many groups initially worked to improve the solvency of graphene sheets by chemical modifications or non-covalent functionalizations [9–12]. With the solution of graphene's dispersibility, these sheets have been used in electrochemistry fields due to their low cost, wide potential window and electrocatalytic activity for a variety of redox reactions. Recently, electrochemiluminescence [13] and electrochemical sensing and biosensing platform based on graphene sheets have been reported by some groups [14,15]. Meanwhile, some groups have employed graphene sheets to determine DA by cyclic voltammetry (CV) [16] and differential pulse voltammetry (DPV) [17]. However, graphene sheets or their based hybrids were few applied to simultaneous determination of AA and DA by CV.

In this paper, a Pt nanoparticles/polyelectrolyte-functionalized ionic liquid/graphene sheets (Pt/PFIL/GS) nanocomposite was synthesized in one pot. The structure and composition of Pt/PFIL/GS nanocomposite were thoroughly studied. Then the Pt/PFIL/GS-modified electrode was fabricated to simultaneously determine AA and DA. Further, the proposed sensor was also applied to determine AA, DA and uric acid (UA) in human urine samples.

2. Experimental

2.1. Materials

1-Methylimidazole (≥98%, Linhai Kaile Chemicals, China) was distilled at reduced pressure before use. Polyethylenimine

* Corresponding author. Tel.: +86 431 8526 2425; fax: +86 431 8526 2800.
E-mail address: lniu@ciac.jl.cn (L. Niu).

0039-9140/$ – see front matter © 2010 Elsevier B.V. All rights reserved.
doi:10.1016/j.talanta.2010.01.061

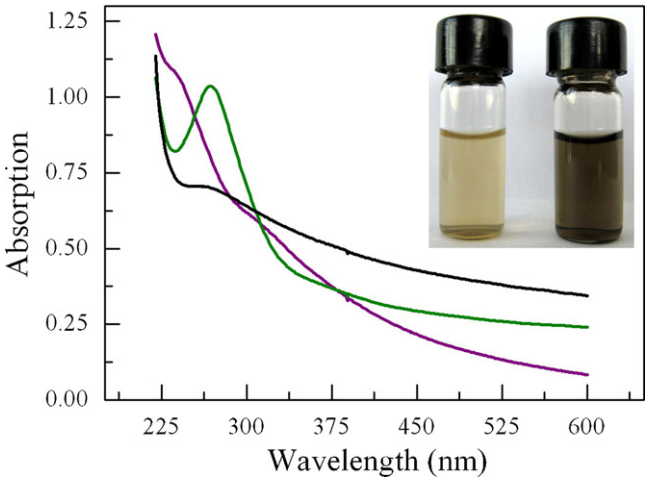

Fig. 1. UV–vis spectra of GO (purple), H_2PtCl_6/PFIL/GO (olive) and Pt/PFIL/GS (black) aqueous solutions. Inset: a photograph of H_2PtCl_6/PFIL/GO (left) and Pt/PFIL/GS (right) nanocomposite solutions. (For interpretation of the references to color in this figure legend, the reader is referred to the web version of the article.)

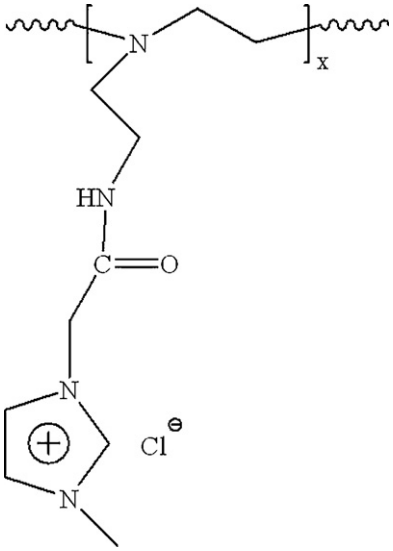

Scheme 1. The molecular structure of PFIL.

(*Mw* = 25,000, Aldrich), graphite powder (spectral requirement, Shanghai Chemicals), $H_2PtCl_6 \cdot 6H_2O$ (≥98%, Shanghai Chemicals), sodium borohydride (99%, Acros), ascorbic acid (≥99.0%, Fluka) and dopamine hydrochloride (Aldrich) were used as received. Urine samples were obtained from healthy laboratory volunteers without any pretreatment, except that they were diluted by 5 times with 0.05 M PBS (pH 7.4). Dialysis membranes (MWCO 10000) were purchased from Sino-American Biotechnology Co. Other reagents were of analytical grades and used as received. All aqueous solutions were prepared with ultra-pure water (>18 MΩ cm) from a Milli-Q Plus system (Millipore).

2.2. Preparation of Pt/PFIL/GS nanocomposite

PFIL was synthesized by our previous method [18]. The scheme of molecular structure of PFIL was shown in Scheme 1. Graphite oxides (GO) were synthesized by a modified Hummers method [19]. A general procedure for the preparation of Pt/PFIL/GS nanocomposite is described as follows. First, 1.0 mg GO was dissolved in 4.0 mL

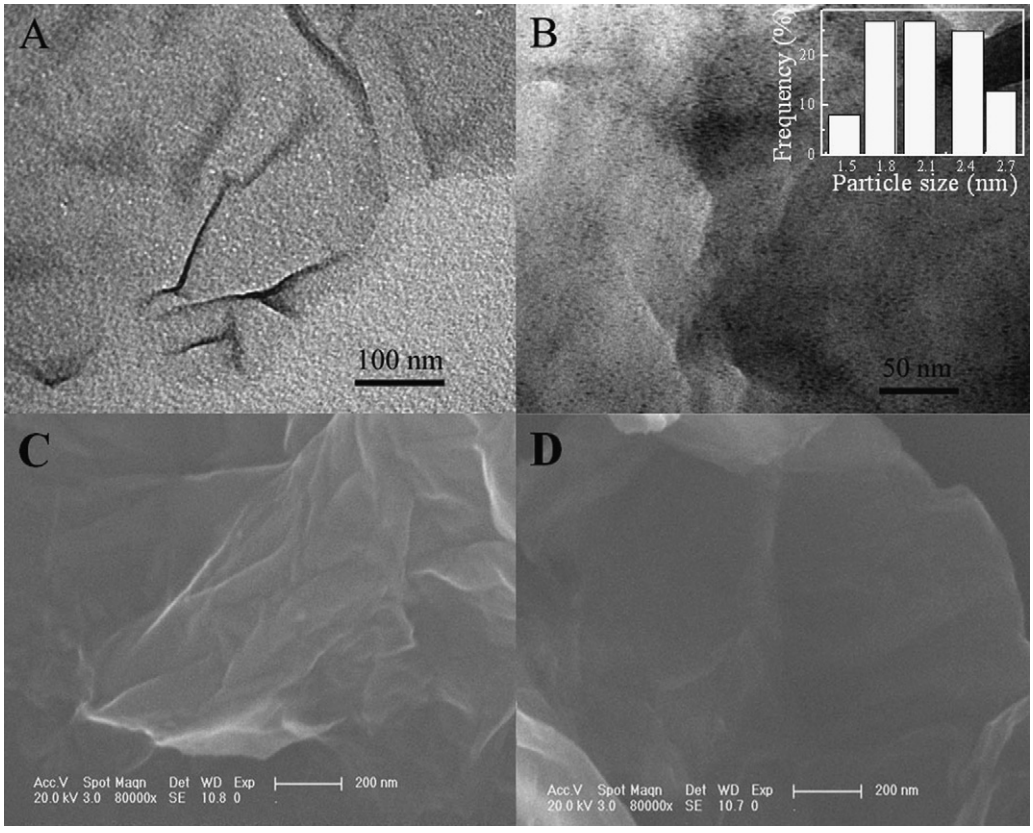

Fig. 2. TEM images of the PFIL/GS (A, sample 1) and Pt/PFIL/GS (B, sample 2) nanocomposite. Inset of B: the particle size distribution of the Pt nanoparticles. SEM images of the PFIL/GS (C, sample 1) and Pt/PFIL/GS (D, sample 2) nanocomposite.

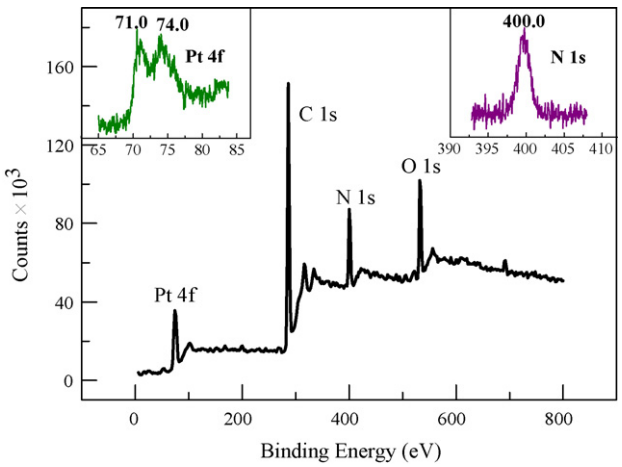

Fig. 3. XPS spectra of the Pt/PFIL/GS (sample 2) nanocomposite. Insets: the Pt 4f doublet (top left) and N 1S (top right).

PFIL aqueous solution (2.0 mg/mL) by ultrasonic treatment. Then an aqueous solution of 50 mM H_2PtCl_6 was added to the above solution under vigorous stirring to give the final concentrations of H_2PtCl_6 of 0, 0.5, 1.0 and 2.5 mM (samples 1, 2, 3, and 4). Subsequently, the pH of this mixture was adjusted to 13.0 using 1 M KOH. Then an excess of freshly prepared $NaBH_4$ solution was rapidly added to the stirred solution, and stirred for 24 h at room temperature. Finally, the sample was collected after thoroughly rinsing with ethanol and deionized water, and vacuum-dried at room temperature.

2.3. Preparation of Pt/PFIL/GS films

The glassy carbon (GC, 3 mm in diameter) electrode was polished subsequently with 1.0, 0.3 and 0.05 μm alumina slurry, sonicated in water for several times, and dried by pure N_2 stream. A drop of Pt/PFIL/GS aqueous solution was dropped onto the clean GC electrode and dried at room temperature.

2.4. Instrument and measurements

Ultraviolet–visible (UV–vis) absorption spectra were recorded using a CARY500 UV/vis/near-IR spectrometer. Transmission electron microscope (TEM) images were obtained using a JEOL 2000 transmission electron microscope operating at 200 kV. Scanning electron microscopy (SEM) measurements were conducted with an XL30 ESEM FEG field emission scanning electron microscope. X-ray photoelectron spectra (XPS) analysis was carried out on an ESCALAB MK II X-ray photoelectron spectrometer. All electrochemical measurements were performed in a three-electrode electrochemical cell using a CHI 660 workstation (CHI Instruments, USA). All experiments were conducted at room temperature.

3. Results and discussion

3.1. Structure characterization

Fig. 1 displays the UV–vis spectra of GO (purple), H_2PtCl_6/PFIL/GO (olive) and Pt/PFIL/GS (black) aqueous solutions. An absorption peak of the GO dispersion appears at ca. 235 nm, which is consistent with previous studies [20]. An absorption peak of H_2PtCl_6 solution alone appears at 258.4 nm. However, in the presence of PFIL, the mixed solution of H_2PtCl_6/PFIL/GO shows a peak at 268 nm, which is attributed to the ligand-to-metal charge-transfer transition of the $[PtCl_6]^{2-}$ ions [21]. After reduction by $NaBH_4$, the peak of $[PtCl_6]^{2-}$ ions disappears, suggesting

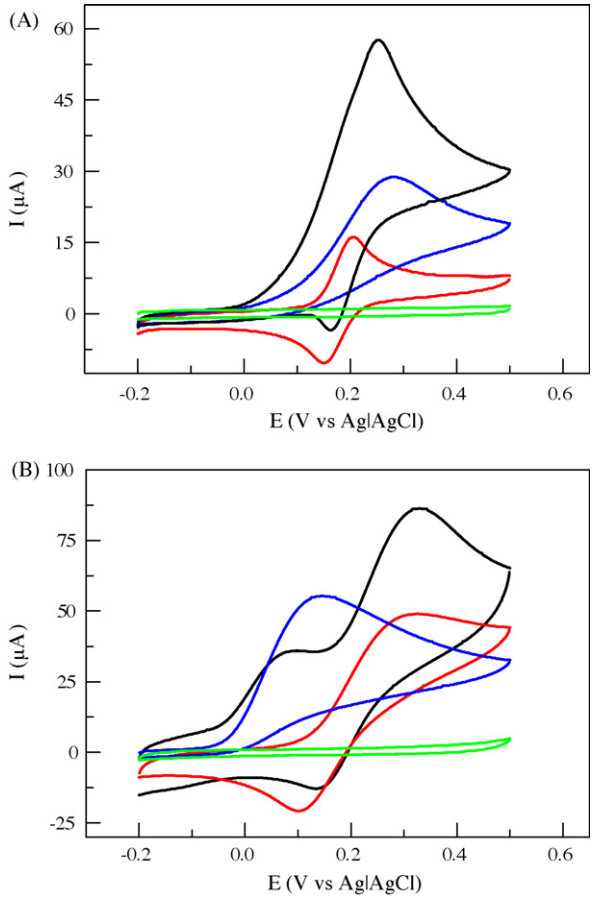

Fig. 4. (A) CV grams recorded at the bare GC electrode in the absence (green) or presence of 1.0 mM DA (red), 2.0 mM AA (blue), 1.0 mM DA and 2.0 mM AA (black). (B) CV grams at the Pt/PFIL/GS-modified GC electrode in 0.05 M N_2-saturated PBS (pH 7.0) without (green) or with 1.0 mM DA (red), 2.0 mM AA (blue), 1.0 mM DA and 2.0 mM AA (black). Scan rate: 0.1 V s^{-1}. (For interpretation of the references to color in this figure legend, the reader is referred to the web version of the article.)

the complete reduction of $[PtCl_6]^{2-}$ ions into Pt nanoparticles. Meanwhile, a broad peak at 262 nm is attributed to the electronic conjugation within the graphene sheets [20]. The inset photograph shows that the color of the solution turns from pale brown to black further confirming the reduction process.

TEM images of the PFIL/GS (A, sample 1) and Pt/PFIL/GS (B, sample 2) nanocomposite are shown in Fig. 2. Pt nanoparticles appear as dark dots on a lighter shaded substrate corresponding to the graphene sheets. In Fig. 2A, there are no dark dots on the translucent PFIL-functionalized graphene sheets. However, Pt nanoparticles occupy part of the surface of graphene sheets with fairly even, non-ordered distribution in Fig. 2B. Moreover, a narrow size-distribution histogram was also obtained from measuring 100 randomly selected particles (inset of Fig. 2B). The diameter of Pt nanoparticles ranges from 1.5 to 2.7 nm, with a mean diameter of 2.1 nm. SEM images of the PFIL/GS (C, sample 1) and Pt/PFIL/GS (D, sample 2) nanocomposite are also shown in Fig. 2.

Fig. 3 shows the XPS spectrum of the Pt/PFIL/GS (sample 2) nanocomposite. The top-left inset represents the XPS signature of the Pt 4f doublet ($4f_{7/2}$ and $4f_{5/2}$) of the resulting Pt nanoparticles. The Pt $4f_{7/2}$ and Pt $4f_{5/2}$ peaks appear at ca. 71.0 and 74.0 eV, which is consistent with previous report on Pt nanoparticles [22]. An exclusively single peak at 400.0 eV (top-right inset) is ascribed to N coordination [23], which confirms the presence of PFIL in the Pt/PFIL/GS hybrid.

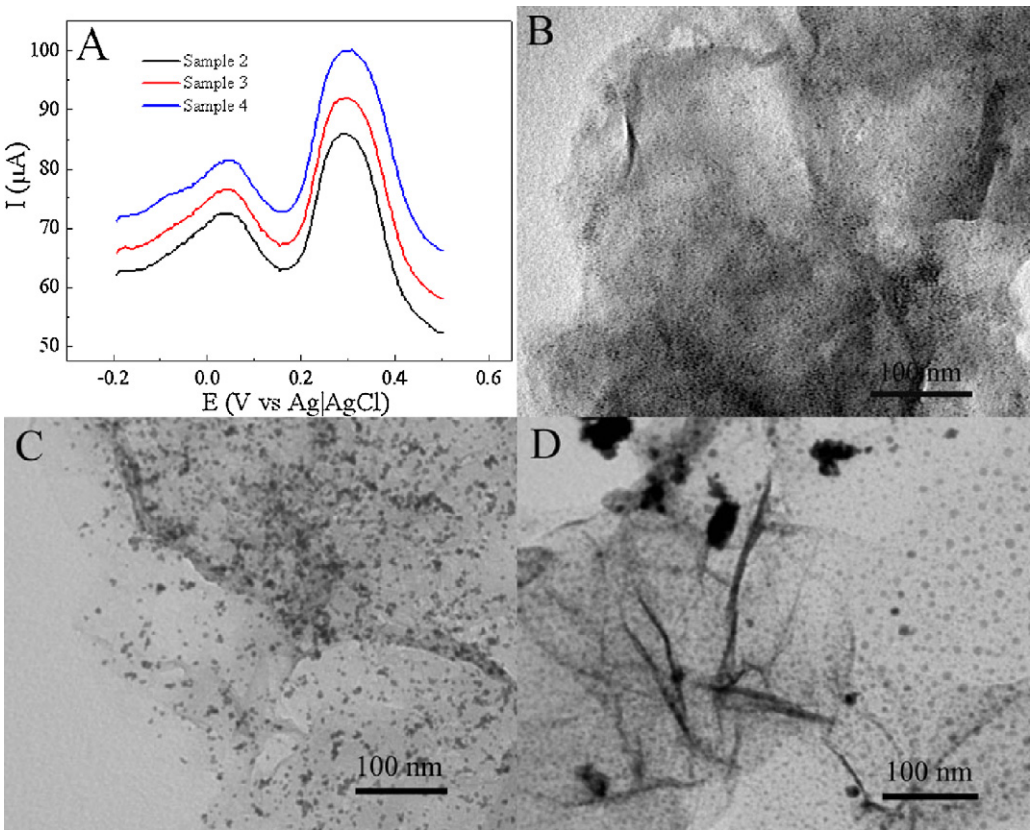

Fig. 5. (A) DPV curves of sample 2 (black line), sample 3 (red line), and sample 4 (blue line). TEM images of (B) sample 2, (C) sample 3 and (D) sample 4. (For interpretation of the references to color in this figure legend, the reader is referred to the web version of the article.)

3.2. Simultaneous electrochemical determination of AA and DA

The electrochemical behaviors of AA, DA and mixture of the two species at the bare GC and such Pt/PFIL/GS (sample 2)-modified electrode are shown in Fig. 4. In Fig. 4A, a peak of AA (blue) and DA (red) oxidation appears at 0.28 and 0.20 V, respectively. The peak potentials of AA and DA almost occur at the sample potential at bare GC electrodes, which leads to the difficult discrimination of the two species [3]. Therefore, a single and sharp peak is observed at 0.25 V (black) at the bare GC electrode in the N_2-saturated phosphate buffer solution (PBS, pH 7.0) containing 2.0 mM AA and 1.0 mM DA (black). The value of its peak current is about the addition of the peak current of AA and DA alone, which further indicates that the overlapping peak of AA and DA is detected at the bare GC electrode. As a control experiment, only low capacitive currents are detected at the bare GC electrode (green) in the N_2-saturated PBS (pH 7.0). In Fig. 4B, the peaks of AA (blue) and DA (red) oxidation appear at about 0.13 and 0.33 V, respectively, at the Pt/PFIL/GS-modified GC electrode. A negative shift of AA oxidation peak and a positive shift of DA oxidation peak result in simultaneous determination of these two species. The difference between the two peak potentials is about 200 mV, which is enough to distinguishing AA from DA (black). Also, only low capacitive currents are detected at the bare GC electrode (green) in the N_2-saturated PBS (pH 7.0).

Up to now, only DA was detected on the graphene-chitosan/GC electrode by Li′ group. However, AA was completely eliminated by the use of graphene-modified electrode [16]. In the contrary, the oxidation of AA was reported on sulfonated polyaniline/graphene-modified GC electrode [24]. It is worthwhile noting that simultaneous determination of AA and DA is achieved at the Pt/PFIL/GS-modified GC electrode. The reasons are concluded in the following aspects. First, molecular structures of DA and AA are distinct from each other. The π–π interaction between phenyl structure of DA and planar hexagonal carbon structure of graphene is attributed to the easy arrival of DA molecules to the surface of modified electrode (Scheme 2A). Second, although the π–π interaction between penta-heterocycle of AA and planar hexagonal carbon structure of graphene is weak, the presence of cationic PFIL provides a remarkable electrostatic attraction to negatively charged AA and rejection to positively charged DA in PBS (pH 7.0) due to the charged characters of AA (pKa = 4.10) and DA (pKa = 8.87). The electrostatic force leads to the realization of AA oxidation on the Pt/PFIL/GS-modified electrode (Scheme 2B). Third, uniform PtNPs might provide synergic influence on the accurate electrochemical determination of AA and DA. The integrated effect of the above three aspects might result in simultaneous determination of AA and DA at the Pt/PFIL/GS-modified GC electrode.

3.3. Influences on electrochemical properties from deposition amount of platinum

Fig. 5A displays the electrochemical properties of three different Pt/PFIL/GS nanocomposite samples (sample 2 black line, sample 3 red line, sample 4 blue line). We can clearly see that the potentials of AA and DA oxidation nearly do not change with the addition of platinum. However, the background current increases due to the increasing of electrode roughness. It indicates that the roughness of graphene sheets is increased by the increasing amount of Pt nanoparticles. The above viewpoint is further confirmed by the TEM images of the three samples (Fig. 5B sample 2, C sample 3, and D sample 4). The Pt nanoparticles grow bigger and bigger from B to D, they even aggregate to very large blocks about 100 nm in Fig. 5D. Because the electrocatalytical properties are not improved

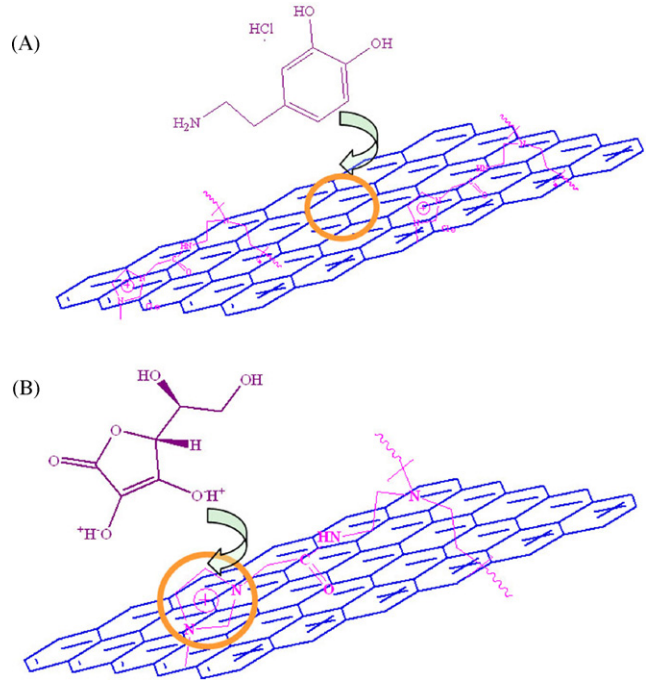

Scheme 2. The reaction mechanism (A) between DA and Pt/PFIL/GS nanocomposite and (B) between AA and Pt/PFIL/GS nanocomposite.

obviously with the addition of Pt amount, and the price of Pt is so high, the sample 2 was used in the following analytical tests.

3.4. Evaluation of the analytical utility of the Pt/PFIL/GS-modified electrodes

To evaluate the analytical utility of the Pt/PFIL/GS-modified electrodes, the detection of increasing concentrations of AA in the presence of DA (Fig. 6A) and the oxidation of continuous addition of DA in the presence of AA (Fig. 6B) were all studied by DPV. Fig. 6A shows the DPV curves for 5 times addition of 1.0 mM AA in the presence of 0.5 mM DA. The current of AA oxidation peak increases with the increase of AA concentration without any change in the DA peak. Similarly, when the concentration of DA is increased in the presence of AA, no significant change in the oxidation current of AA is observed (Fig. 6B). These results suggest that the Pt/PFIL/GS-modified GC electrode can be utilized for the determination of AA in the presence of DA and vice versa. Therefore, the Pt/PFIL/GS nanocomposite has a great potential for the application in the AA and/or DA detection in real samples.

The proposed sensor in real sample analysis was also examined in human urine samples. As known, the concentration of UA in normal human urine samples is 2.4–4.1 mM, so after the urine samples were diluted by 5 times, the concentration of UA is 0.5–0.8 mM in our test samples. From Fig. 7, it can be seen that the oxidation peaks of AA, DA and UA appear at about 0.09, 0.32 and 0.46 V, respectively, in human urine samples containing 1 mM AA and 1 mM DA. The inset graph is the DPV curve recorded in urine samples without addition of AA and DA. A single peak of UA is observed at about 0.46 V, which is consisted with the result of the urine samples with AA and DA.

The reproducibility of electrochemical sensor construction was estimated from the response to a same sample at five electrodes prepared under the same conditions. The reproducibility is satisfying with a RSD of 4.95%. The operational reproducibility of the sensor was measured by a same Pt/PFIL/GS-modified electrode's continuous response to a same sample. The RSD is 2.73% for continuous six-time determinations. The electrochemical sensor exhibits high stability, its voltammetric response remains stable even after continuous scanning for 50 cycles. After 1-month storage at room temperature, the response current of the sensor almost does not decrease in 0.05 M PBS containing 2.0 mM AA and 1.0 mM DA. The good stability of the Pt/PFIL/GS-based sensor might be mainly attributed to the presence of PFIL in the composite. First, polymer chains of PFIL could effectively maintain the micro-structure of

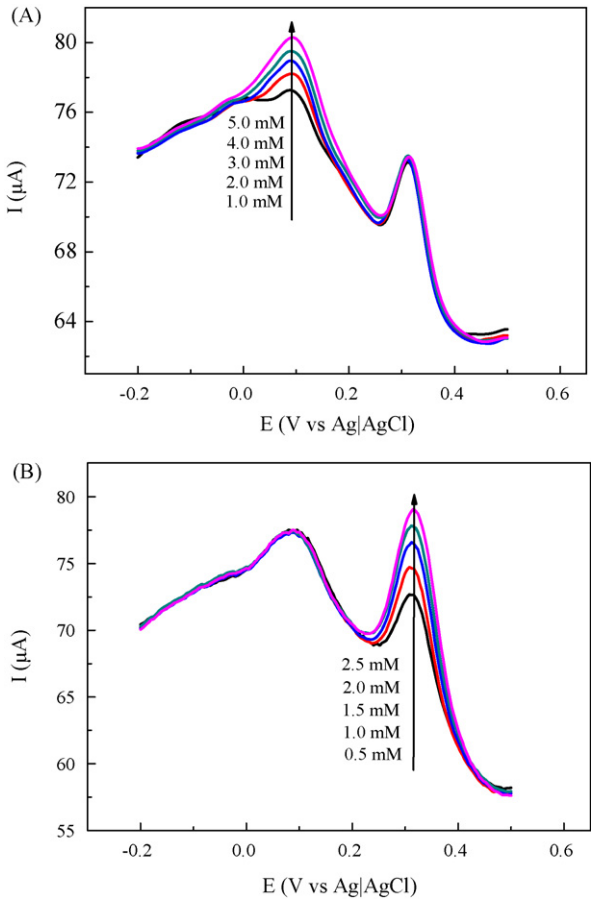

Fig. 6. (A) DPV curves for AA 1.0, 2.0, 3.0, 4.0, and 5.0 mM from inner to outer in the presence of 0.5 mM DA. (B) DPV curves for DA 0.5, 1.0, 1.5, 2.0, and 2.5 mM from inner to outer in the presence of 1.0 mM AA. The blank solution is 0.05 M N_2-saturated PBS (pH 7.0).

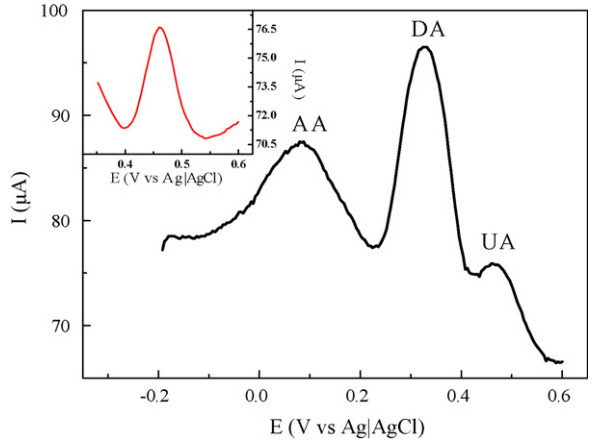

Fig. 7. DPV curve of urine samples containing 1.0 mM AA and 1.0 mM DA. Inset: DPV curve of urine samples without AA and DA.

Pt/PFIL/GS nanocomposite, and help to form a uniform dry film. Second, polymer chains of PFIL could also prevent the Pt/PFIL/GS membrane shedding from electrode during the analytical tests [14]. The Pt/PFIL/GS-modified electrode can be used over 50 times without any film shedding, which greatly reduces the cost of tests. Therefore, the Pt/PFIL/GS nanocomposite could be promisingly applied to determine AA and DA concentration in the practical clinical analysis.

4. Conclusions

In conclusion, the Pt nanoparticles were coupled on PFIL-functionalized graphene sheets in one step. Moreover, the Pt/PFIL/GS-modified electrode was fabricated to simultaneously determine AA and DA. The difference between the peak potentials is over 200 mV, which is enough to distinguishing AA from DA. The DPV results confirm that the existence of one does not affect the determination of the other. Three independent oxidation peaks appear at Pt/PFIL/GS-modified electrodes in human urine samples containing AA and DA. The life time and reproducibility of Pt/PFIL/GS-modified electrodes are all very satisfying. Therefore, the Pt/PFIL/GS nanocomposite might offer a good possibility for applying it to routine analysis of AA and DA in clinical use.

Acknowledgements

This work was financially supported by the National Natural Science Foundation of China (Nos. 20673109 and 20827004) and Chinese Academy of Sciences (Nos. KGCX2-YW-231 and YZ200906).

References

[1] D.R. Shankaran, K. Iimura, T. Kato, Sens. Actuators B 94 (2003) 73.
[2] P. Ramesh, G.S. Suresh, S. Sampath, J. Electroanal. Chem. 561 (2004) 173.
[3] A.P. dos Reis, C.R.T. Tarley, N. Maniasso, L.T. Kubota, Talanta 67 (2005) 829.
[4] K.S. Prasad, G. Muthuraman, J.-M. Zen, Electrochem. Commun. 10 (2008) 559.
[5] N. Jia, Z. Wang, G. Yang, H. Shen, L. Zhu, Electrochem. Commun. 9 (2007) 233.
[6] M. Ates, J. Castillo, A.S. Sarac, W. Schuhmann, Microchim. Acta 160 (2008) 247.
[7] Y. Zhao, Y. Gao, D. Zhan, H. Liu, Q. Zhao, Y. Kou, Y. Shao, M. Li, Q. Zhuang, Z. Zhu, Talanta 66 (2005) 51.
[8] D. Li, R.B. Kaner, Science 320 (2008) 1170.
[9] Y. Si, E.T. Samulski, Nano Lett. 8 (2008) 1679.
[10] Y. Liang, D. Wu, X. Feng, K. Müllen, Adv. Mater. 21 (2009) 1.
[11] S. Stankovich, R.D. Piner, X. Chen, N. Wu, S.T. Nguyen, R.S. Ruoff, J. Mater. Chem. 16 (2006) 155.
[12] X. Fan, W. Peng, Y. Li, X. Li, S. Wang, G. Zhang, F. Zhang, Adv. Mater. 20 (2008) 4490.
[13] H. Li, J. Chen, S. Han, W. Niu, X. Liu, G. Xu, Talanta 79 (2009) 165.
[14] C. Shan, H. Yang, J. Song, D. Han, A. Ivaska, L. Niu, Anal. Chem. 81 (2009) 2378.
[15] H. Wu, J. Wang, X. Kang, C. Wang, D. Wang, J. Liu, I.A. Aksayb, Y. Lin, Talanta 80 (2009) 403.
[16] Y. Wang, Y. Li, L. Tang, J. Lu, J. Li, Electrochem. Commun. 11 (2009) 889.
[17] S. Alwarappan, A. Erdem, C. Liu, C.-Z. Li, J. Phys. Chem. C 113 (2009) 8853.
[18] F. Li, C. Shan, X. Bu, Y. Shen, G. Yang, L. Niu, J. Electroanal. Chem. 616 (2008) 1.
[19] N.I. Kovtyukhova, P.J. Ollivier, B.R. Martin, T.E. Mallouk, S.A. Chizhik, E.V. Buzaneva, A.D. Gorchinskiy, Chem. Mater. 11 (1999) 771.
[20] D. Li, M.B. Müller, S. Gilje, R.B. Kaner, G.G. Wallace, Nat. Nanotechnol. 3 (2008) 101.
[21] T. Teranishi, M. Hosoe, T. Tanaka, M. Miyake, J. Phys. Chem. B 103 (1999) 3818.
[22] F. Li, F. Li, J. Song, J. Song, D. Han, L. Niu, Electrochem. Commun. 11 (2009) 351.
[23] A.E. Shalagina, Z.R. Ismagilov, O.Y. Podyacheva, R.I. Kvon, V.A. Ushakov, Carbon 45 (2007) 1808.
[24] H. Bai, Y. Xu, L. Zhao, C. Li, G. Shi, Chem. Commun. (2009) 1667.